Validation of Brightness Temperatures observed by SAPHIR instrument onboard Megha-Tropiques Satellite

Gaëlle CLAIN, Hélène Brogniez

LATMOS-IPSL, 11, boulevard d'Alembert, 78280 Guyancourt, France

Abstract

The SAPHIR (Sondeur Atmosphérique du Profil d'Humidité Intertropicale par Radiométrie) instrument onboard the Megha-Tropiques (MT) satellite observes the tropical atmosphere since October 2011. It is a cross track scanning sounder with 6 channels in the 183.31 GHz water vapour absorption band and a resolution of 10km at nadir.
This work investigates the concordance of SAPHIR brightness temperatures (BT) with regards to BTs simulated from reference Vaïsala RS92-SGPD radiosonde observations performed during the CINDY/DYNAMO (sept. 2011 to March 2012) tropical campaign and collocated with MT observations. The radiosonde observations were subject to a quality control procedure with the ASPEN software, and to a upper tropospheric dry bias correction specific to the Vaïsala RS92 probes. which was either developed by the GRUAN community or by the constructor. The radiosonde observations were subject to a quality control procedure with the ASPEN software, and to a upper tropospheric dry bias correction specific to the Vaïsala RS92 probes. The RTTOV v10 radiative model is then used to simulate equivalent SAPHIR BTs from the radiosonde profiles. The difference between simulated and observed brightness temperatures are investigated so as to be related to observation predictors of SAPHIR, radiosonde measurement accuracy and radiative model performance.

INTRODUCTION

Water vapour is the most important greenhouse gas and its impact on the earth radiative balance is governed by the spatiotemporal complexity of its distribution and the different phases under which water exists in the atmosphere. In order to describe the mechanisms driving the distribution of water vapour and clouds, long term observations with high temporal and spatial resolutions are required. The Indo-French Megha-Tropiques satellite, launched in October 2011, is the first satellite dedicated to the observation of the water cycle and energy budget in the tropics, with a daily average overpass frequency greater than 3 between 20°S and 20°N.

The objective of this paper is to evaluate the SAPHIR brightness temperature (BT) observations using reference measurements from radiosoundings. The first section describes the radiosonde dataset used as reference and the methodology for radiative transfer simulations. The second section discusses the influences that can exert on the difference between observed and simulated BTs.

1 DATA AND METHODOLOGY

1.1 RADIOSONDE OBSERVATIONS

Vaïsala RS92 radiosonde observations of relative humidity (RH) are chosen as reference observations. The collocated RH observations are used as an input to a radiative transfer model (RTTOV-v10, Saunders et al., 1999, see section 1.3) in order to simulate BTs as seen by SAPHIR instrument channels.
The radiosonde observations used in this study were performed at 11 tropical sites (summarized in Table 1) during the CINDY/DYNAMO campaign between September 2011 and March 2012 in the

Indian Ocean. 98% of the observations were performed in oceanic conditions. The purpose of this campaign was to document the influence of intra seasonal variability (i.e. Madden Julian Oscillations) on climate.

The uncertainties and errors related to RS92 are well documented (Milosevich et al., 2009, Vömel et al., 2007) and correction methods have been developed (Wang et al.,2012). Indeed, while widely used during scientific campaigns, RS92 humidity observations are affected by :

- A solar radiative bias affecting only daytime observations.
- A time lag error that induces a slower sensor response at lower temperatures. This error becomes significant for temperatures lower than -45°C.
- A sensor random production variability related to humidity conditions, ranging ±1.5% of the measured RH for RH>10% and ±3% of the measured RH for RH<10%.
- A residual uncertainty bias accounting for both sensor and ground check calibration variability that differs between daytime ± (5% of the measured RH + 0.5% RH offset) and night time ±(4% of the measured RH ± 0.5% RH offset).
-

The radiosonde dataset was submitted to a quality control procedure with the Atmospheric Sounding Processing Environment (ASPEN) software (Ciesielsky et al. 2011) and includes two types of correction procedures: a correction developed and applied by the constructor through the acquisition system and a correction developed in the framework of GCOS Reference Upper Air Network (GRUAN, Seidel et al. 2009) community. The Vaïsala correction accounts for the dry bias and time lag error. In addition to these, the GRUAN correction accounts for calibration uncertainties (Wang et al. 2012). Figure 1 shows that the contribution of the two corrections are sensitively equally distributed in the database.

1.2 SAPHIR OBSERVATIONS

The Sondeur Atmosphérique du Profil d'Humidité Intertropicale par radiométrie (SAPHIR, Eymard et al., 2002) sounds the tropical atmosphere with 6 channels near the 183.31GHz water vapour absorption line. SAPHIR channels specifications are shown in Table 2. Hereafter SAPHIR channels will be referred to as C1 to C6 with respect to Table 2 specifications. This study evaluates level 1A2 BTs which is a re-sampling of the initial 182 overlapping pixels per scan of SAPHIR, thus providing 130 contiguous pixels per scan. SAPHIR BTs are filtered according to the method stated in Hong et al. (2005) in order to reject deep convective and precipitating scenes.

The collocated radiosonde observations correspond to a time window of ±45 minutes between the radiosonde launch and the satellite overpass, and a distance inferior to 50km between the radiosonde launch site and SAPHIR closest pixel.

1.3 RADIATIVE TRANSFER SIMULATIONS

The Radiative Transfer for TIROS Operational Vertical Sounder (RTTOV) code is a fast radiative transfer model (Saunders et al., 1999, Matricardi et al., 2004) that simulates satellite radiances from thermodynamic profiles (pressure (hPa) , temperature (K) and specific humidity (kg/kg)) using the radiometer zenithal angle. The emissivity is either extracted from an atlas elaborated using SSMI measurements (Prigent et al. 2008) for continental areas or computed by the FASTEM-4 (English & Hewison, 1999) over the oceans.

2 RESULTS AND DISCUSSION

2.1 BIAS FEATURES

Table 3 shows the mean difference (hereafter named "BT bias") and standard deviations between simulated and observed BTs for each SAPHIR channel. Considering the full dataset BT bias (i.e. day and night): for C1, observed BTs are warmer in average than the simulated BTs by 0.45K. For C2 to

C6, observed BTs are colder in average than the simulated BTs. The BT bias increases from C2 to C6, peaking for C6 by 2.6 K.

Figure 2 shows a temperature dependence of the simulated – observed BT bias with respect to SAPHIR observed BTs, with a decreasing spread and increasing mean difference from cold (C1) to warm (C6) conditions. Observations in conditions colder than 270 K for C6 show a larger bias. These observations are compatible with cloudy scenes that have not been removed from the SAPHIR data. The removal of those cloudy points decreases the mean bias by less than 1 K (not shown).

2.2 INVESTIGATIONS OF POSSIBLE BIAS SOURCES

The possible sources of bias can be linked to (i) the SAPHIR instrument itself, (ii) the radiosonde observations and (iii) the radiative model.

(i) SAPHIR observations are affected by the limb effect, described in Buehler et al. (2004): the BTs scanned at nadir are warmer in average than the BTs scanned at the edge of swath. On a single orbit, the mean BT difference between nadir and edges of swath has been verified to range between 5K for C1 and 4 K for C6. Figure 3 shows that restricting the dataset to zenithal angles close to nadir has a minor impact on the mean bias (<0.2K).

(ii) Concerning the radiosonde observations, a possible site-to-site dependence is analysed. Mean biases and standard deviations are computed for each site. Figure 4 shows that the bias ranges are fairly coherent amongst the radiosonde launch sites. One can notice that the bias computed from radiosonde observations performed at Nairobi site (NAI) shows a greater amplitude than for the other sites on C2 (183±1.1GHz) but NAI observations only account for 2% of the dataset (Figure 3), therefore minimizing its impact on the overall statistics.

With regards to the accuracy of radiosonde measurements:
- The daytime radiosonde observations are subject to radiative bias and time lag errors that are corrected.
- Half of the daytime dataset is also corrected for calibration errors with the GRUAN correction (figure 3).

Therefore a large share of the dataset is affected by the production and calibration variabilities: night-time observations and half of daytime observations. Table 3 shows the mean BT bias and standard deviation for daytime and night-time subsets. The difference between the two subsets is small (0.1K) for C2 to C6 and peaks by 0.5K for C1.

In order to evaluate the sensitivity of SAPHIR BT simulations with RTTOV-v10 to daytime calibration variability only, relative humidity input profiles are artificially modified according to its extreme values (section 1.1). Figure 5 shows the sensitivity of RTTOV-v10 simulations for SAPHIR BTs to this change. Note that an increase (resp. decrease) of RH% profile drives to a decrease (resp. increase) in simulated BTs amplitudes. The results for C1 only are not representative since the variability of changes for C1 has the same order of amplitude as the amplitude of BT change in Kelvins due to the input perturbation of RH%. For C2 to C6 the total sensitivity of the model is close to 1K. Although this sensitivity is quite large compared to the simulated – observed BT bias, this source of variability does not counteract the bias temperature dependant pattern discussed above.

(iii) The performances of RTTOV are evaluated against the Atmospheric Radiative Transfer Simulator (ARTS, Buehler et al. 2005). Figure 6 shows ARTS and RTTOV-v10 BT biases by normalised distributions and statistical keys for each SAPHIR channel. For C1 to C4, the two models are in good agreement. The BT bias computed from ARTS simulations is relatively smaller in average for C5 (1.3K) and C6 (1.9K) . Although the difference between the two models maximises for C6 by 0.7K, this exercise gives a good confidence in RTTOV-v10 performances for SAPHIR BTs simulations.

3 CONCLUSIONS

In order to compare SAPHIR observed brightness temperatures to reference brightness temperatures, a set of Vaïsala RS92 humidity profiles are used as input to the fast radiative transfer model RTTOV-V10. The BT bias show a temperature dependant pattern: the bias amplitude increases from cold (C1) to warmer (C6) physical conditions.
Investigations do not show any evidence of dependence to the instrument zenithal angle, nor a bias due to the contribution of a specific observation site. The sensitivity of the model to calibration variability of radiosonde observations, yet 1K large for C2 to C6, does not explain the temperature dependant pattern observed for the bias.
Finally, the evaluation of RTTOV simulations with regards to ARTS LBL model tends to discard a poor performance of the model. Further work within the X-CAL working group of Global Precipitation Measurement (GPM) mission includes an additional comparison of RTTOV simulations to the MonoRTM radiative transfer model (Payne et al., 2008), and a strengthening of filter processes in order to strictly restrict the comparisons to clear sky scenes.

IMAGES AND TABLES

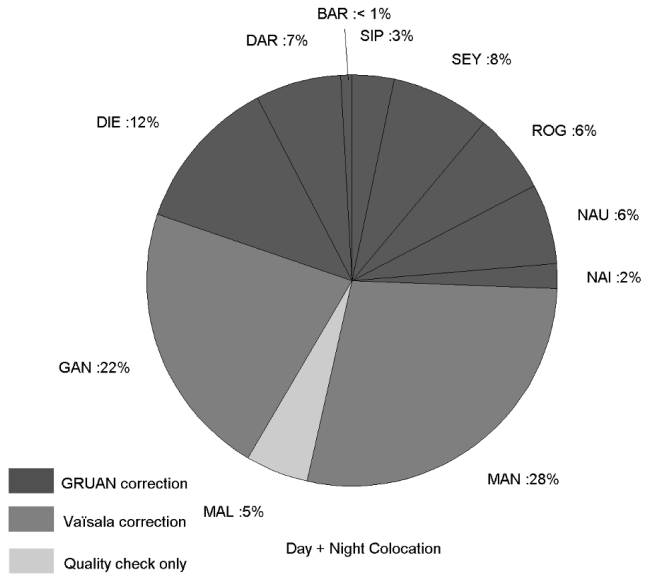

Figure 1: **Contribution of each site to the total number of radiosonde observations. Grey shades refer to the type of correction applied to the radiosonde observations.**

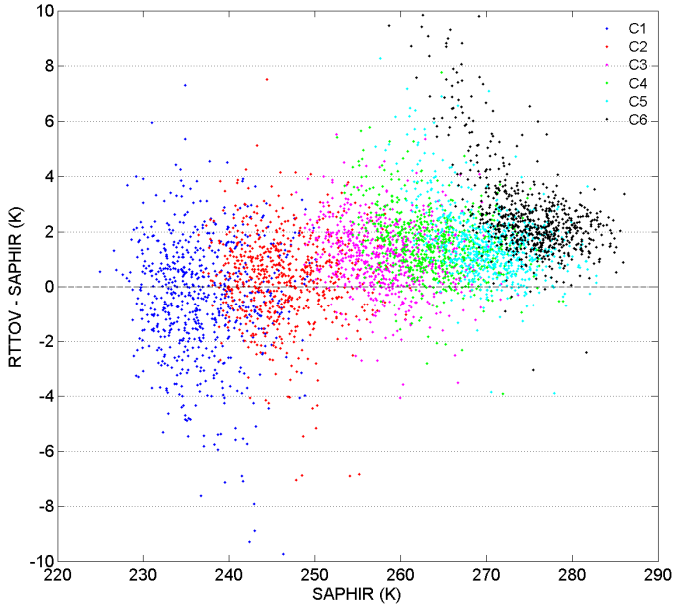

Figure 2: **RTTOV-SAPHIR brightness temperature bias (K) dependence to observed SAPHIR brightness temperatures.**

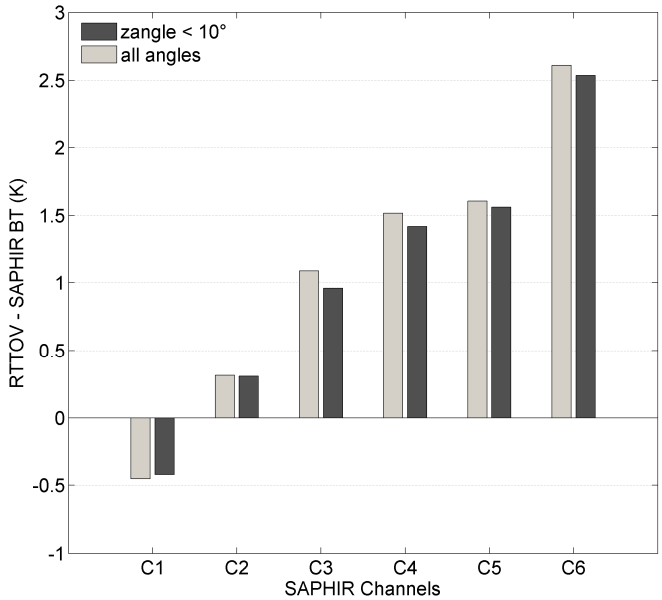

Figure 3: **RTTOV-SAPHIR brightness temperature bias (K) dependence to zenithal angle.**

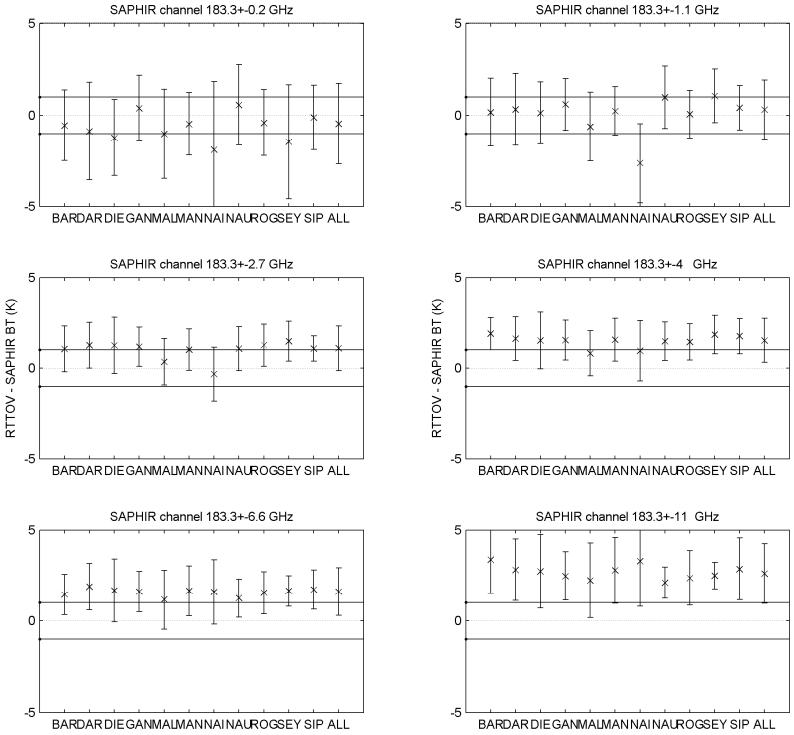

Figure 4: **RTTOV-SAPHIR brightness temperature bias (K) for each saphir channel and each Cindy - Dynamo radisonde launch site used in the database. Errorbars depict standard deviations (K) restricted to a single site.**

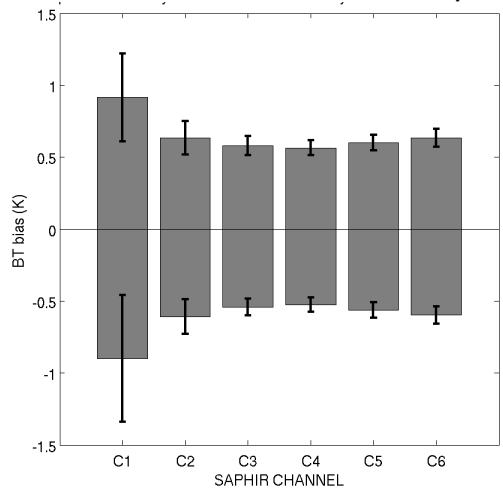

Figure 5: **Sensitivity of RTTOV radiative transfer model to a perturbation of the input RH profile according to the extreme values of the calibration uncertainty for daytime observations. Grey bars show the mean output BT change (K) with regards to reference simulation, black errorbars show the standard deviation (of change in output BT (K) with regards to reference simulations.**

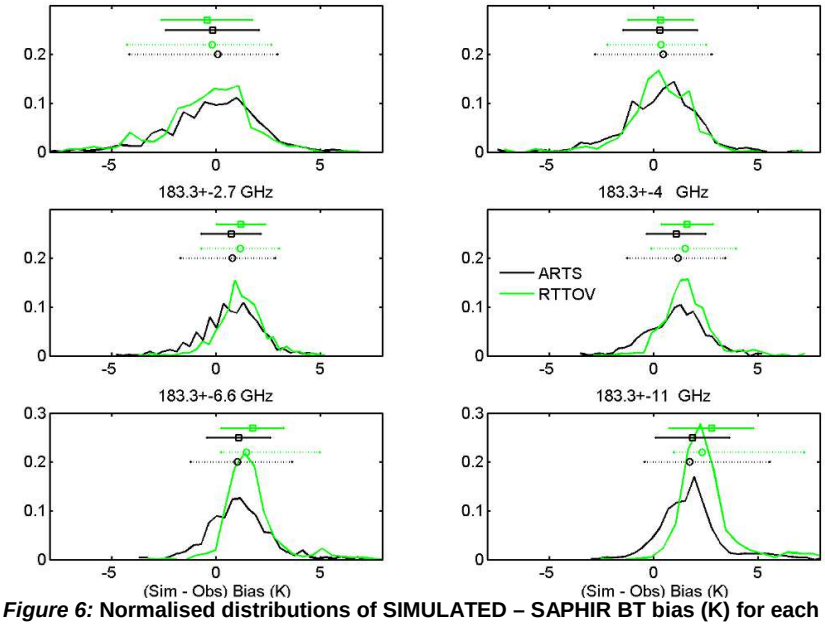

Figure 6: **Normalised distributions of SIMULATED – SAPHIR BT bias (K) for each SAPHIR channel, RTTOV (green lines) and ARTS (black lines). Square marks and plain lines show mean and standard deviation. Circle marks and dotted lines show median, 5th and 95th centiles.**

site acronym	site name	country / flag	elevation (m)	latitude	longitude	site type
BAR	Baruna Jaya	Indonesia	3.0	-7 to -6.43	95 to 99.52	R/V
DAR	Darwin	Australia	30.0	130.89	-12.42	continental
DIE	Diego Garcia	UK	2.0	72.42	-7.31	oceanic
GAN	Gan Island	Maldives	1.0	73.15	-0.69	oceanic
MAL	Male	Maldives	2.0	73.53	4.19	oceanic
NAI	Nairobi	Kenya	1795.0	36.76	-1.3	continental
NAU	Nauru	Nauru Island	4.0	166.92	-0.52	oceanic
ROG	Roger Revelle	U.S.A.	19.0	-29.85 to 4.88	36.39 to 91.45	R/V
SEY	Seychelles	Seychelles	4.0	-4.68	55.53	oceanic
SIP	Sipora	Indonesia	7.0	99.58	-2.03	oceanic
MAN	Manus	Manus Island	4.0	-2.060	147.430	oceanic

Table 1: **List of the CINDY/DYNAMO radiosonde launch sites with specification of site acronyms (1st column), coordinates (columns 4 to 6), and site type (last column). R/V site type refers to Research Vessel**

	Central Frequency	Bandwidth (MHz)	NE DT (K)
C1	**183.31 +- 0.2 GHz**	200	1.36
C2	**183.31 +- 1.1 GHz**	350	1
C3	**183.31 +- 2.8 GHz**	500	0.86
C4	**183.31 +- 4 GHz**	700	0.72
C5	**183.31 +- 6.6 GHz**	1200	0.57
C6	**183.31 +- 11 GHz**	2000	0.5

Table 2: **Radiometric in-flight performances of SAPHIR Channels with specification of Channel central frequency (Hz) and Bandwidth (MHz).**

	day + night		day		night	
	Bias (K)	σ (K)	Bias (K)	σ (K)	Bias (K)	σ (K)
C1	-0.45	2.2	-0.2	2.3	-0.7	2
C2	0.3	1.6	0.3	1.7	0.3	1.5
C3	1	1.2	1.1	1.2	1	1.2
C4	1.5	1.2	1.6	1.2	1.5	1.2
C5	1.6	1.3	1.7	1.3	1.5	1.3
C6	2.6	1.6	2.7	1.6	2.5	1.6

Table 3: **RTTOV-SAPHIR brightness temperature bias (K) and standard deviation (K) for each SAPHIR channel. The bias computed from the complete dataset, daytime and nighttime subsets are displayed left to right.**

REFERENCES

Buehler, S. A., Kuvatov, M., John, V. O., Leiterer, U. and Dier,H., (2004) Comparison of microwave satellite humidity data and radiosonde profile: a case study. J. Geophys. Res., **109**, D13103, doi:10.1029/2004JD004605.

Buehler, S. A., P. Eriksson, T. Kuhn, A. von Engeln and C. Verdes (2005) ARTS, the Atmospheric Radiative Transfer Simulator, *J. Quant. Spectrosc. Radiat. Transfer*, *91*(1), 65-93, doi:10.1016/j.jqsrt.2004.05.051.

Ciesielski, P. E., Haertel, P. H., Johnson, R. H., Wang, J., and Loehrer, S., (2011): Developing High-Quality Field Program Sounding Datasets. *Bull. Amer. Met. Soc.*, **93**, 325-336.

English, S. and Hewison, T.: A fast generic millimeter-wave emissivity model, Proceedings of SPIE, 3503, 288-300, 1999.

Eymard L., M. Gheudin, P. Laborie, F. Sirou, C. Le Gac, J.P. Vinson, S. Franquet, M. Desbois, F. Karbou, R. Roca, N. Scott, P. Waldteufel (2002) The SAPHIR humidity sounder, *Instrumental Notes of IPSL n°24, ISSN 1626-8334.*

Hong, G., Heygster, G., Miao, J., Kunzi, K.(2005) Detection of tropical deep convective clouds from AMSU-B water vapor channels measurements. J. Geophys. Res., **110**, D05205, doi:10.1029/2004JD004949.

Matricardi, M, Chevallie,r F, Kelly, G, Thépaut, J-N. (2004) An improved general fast radiative transfer model for the assimilation of radiance observations. *Q. J. R. Meteorol. Soc.,* **130**, 153–173.

Miloshevich, L. M., Vömel, H., Whitman, D. N., and Leblanc, T., (2009) Accuracy assessment and correction of Vaisala RS92 radiosonde water vapor measurements. *J. Geophys. Res.,* **114**, D11305, doi:10.1029/2008JD011565.

Payne, V. H. , Delamere, J. S., Cady-Pereira, K. E., Gamache, R. R., Moncet, J-L., Mlawer, E. J. and Clough, S. A., (2008) , "Air-broadened halfwidths of the 22 GHz and 183 GHz water vapor lines", *IEEE Trans. Geosci. Remote Sens*., **46** (11), 3601-3617.

Prigent C., Jaumouille, E., Chevallier, F., and Aires, F. (2008) A parameterization of the Microwave land surface emissivity between 19 and 100 GHz, anchored to satellite – derived estimates, *IEEE Trans. Geosci. Remote Sens.*, **46**, 344-352.

Saunders R.W., Matricardi, M. and Brunel, P. (1999a): A fast radiative transfer model for assimilation of satellite radiance observations - RTTOV-5. *ECMWF Research Dept. Tech. Memo.* **282.**

Seidel, Dian J., and Coauthors (2009) Reference Upper-Air Observations for Climate: Rationale, Progress, and Plans. *Bull. Amer. Meteor. Soc.*, **90**, 361–369.

Vömel, H., Selkirk, H., Milosevich, L., Valverde-Canossa, J., Valdés, J., Kyrö, E., Kivi, R., Stolz, W., Peng, G., and Diaz, J. A. (2007) Radiation Dry Bias of the Vaïsala RS92 Humidity Sensor, Journal of Atmospheric and Oceanic Technology., **24**, pp. 953-963, doi: 10.1175/JTECH2019.1.

Wang, J., Zhang, L., Dai, A., Immler, F., Sommer, M. and Voemel, H., (2012) Radiation dry bias correction of Vaisala RS92 humidity data and its impacts on historical radiosonde data. J. Atmos. Oceanic Technol., **30**, 197-214.